ASIAN JOURNAL OF CIVIL ENGINEERING (BUILDING AND HOUSING) VOL. 10, NO. 2 (2009)
PAGES 163-176

A KINEMATIC LIMIT APPROACH FOR THE STABILITY ANALYSIS OF NAILED SOIL SLOPES

D. Giri* and A. Sengupta
Department of Civil Engineering, IIT-Kharagpur, Kharagpur, W.B. 721302, India

Abstract

An analytical method is presented based on the kinematic theorem of limit analysis applied to the stability of reinforced slopes under the seismic loading condition. The rate of external work is due to soil weight and inertia force induced by the earthquake and the only contribution to energy dissipation is that provided by the reinforcement. In the present analysis a rotational failure mechanism is considered. The proposed method considered a log-spiral failure surface. In order to verify the proposed method of analysis; two published case studies Clouterre Test Wall No. 1 and the 4.5 m high wall known as Eparris Wall, built to retain a little cut in plastic clay are utilized. The probable failure surface and the factor of safety obtained by the proposed method are found to be in good agreement with the published test results. Finite element numerical modeling by FLAC is done for these test walls. Numerical analysis is found to be good agreement with the published results and also with field observations.

Keywords: Kinematic theorem; limit analysis; reinforced slope; earthquake; log-spiral failure surface; factor of safety.

1. Introduction

There are several methods currently available for the design of nailed soil slopes, such as the German method. (Stocker et al. [1]), the Davis method. (Mitchell and Villet,[2]), the method developed by Gassler and Gudehus [3,4]. The French method, (Schlosser, [5]), and the finite element method, (Dawson et al. [6] Griffiths et al. [7]). An analytical method is presented here based on the kinematics theorem of limit analysis [8, 9 and10] applied to study the stability of reinforced slopes under the seismic loading condition. The kinematic theorem states that slope will collapse if the rate of work done by external loads and body forces exceed the energy dissipation rate for any assumed kinematically admissible failure mechanism. Soil deformation is assumed to be plastic and failure is associated with the Coulomb yield condition.

In the present approach, the following assumptions are made:

1. The effect of pore pressure build-up and change of soil strength due to earthquake

* E-mail address of the corresponding author: Email: debagiri@rediffmail.com (D. Giri)

shaking are ignored.

2. The reinforcement layers are finite in number and have same length.

3. The resistance to bending, shear and compression is ignored.

4. The deformation of the soil in the active zone is sufficient to fully mobilize the shear strength of the soil over the entire failure surface.

5. The failure is along a surface defined by a logarithmic spiral passing through the toe of the slope and intersects the ground at right angle. The centre of the spiral is located on a straight line which rises at an angle ϕ.

Under these assumptions, the reinforcements provide tensile forces. The rate of external work is due to soil weight and inertia force induced by the earthquake and the contribution to energy dissipation is that provided by the reinforcement and cohesion of soil.

2. Method of Analysis

A kinematic limit theorem applied to the stability analysis of nailed soil slopes is presented in this study. This approach is based on the upper bound theorem of plasticity. It is assumed in kinematic approach of limit analysis that the soil is perfectly plastic and its deformation is governed by associated flow rule. Mathematically,

$$\dot{\varepsilon}_{ij}^{pl} = \lambda \frac{\partial f(\sigma_{ij})}{\partial \sigma_{ij}} \quad \lambda \geq 0 \quad \text{if } f = 0 \text{ and } \quad \lambda = 0 \text{ if } f < 0 \tag{1}$$

Where $\dot{\varepsilon}_{ij}^{pl}$ is the plastic strain rate tensor in a kinematic admissible velocity field, σ_{ij} is the stress tensor associated with strain rate tensor ε_{ij},. λ is a non-negative scalar multiplier and $f(\sigma_{ij}) = 0$ is the yield criteria. Mohr-coulomb failure criteria is assumed and the discontinuity vector (velocity jump) must be inclined to the rupture surface at angle of internal friction ϕ.

The kinematic theorem of limit analysis states that when the rate of work done by the external forces and body forces exceeds the rate of internal energy dissipation, the structure will collapse.

Drucker et al. [11] represented mathematically this theorem as

$$\int_V \sigma_{ij} \dot{\varepsilon}_{ij} dV \geq \int_S T_i v_i dS + \int_V \gamma_i v_i^* dV \tag{2}$$

The left hand side of the equation represents the rate of energy dissipation during an incipient failure of a structure and the right hand side includes the rate of work done by all the external forces. T_i is the stress vector on the boundaries S and v_i is the velocity vector on loaded boundary S. γ_i is the specific weight vector and v_i^* is the velocity in the volume V.

The mathematical form of the theorem states that the rate of energy dissipation is not less

than the rate of work done of external forces in any kinematically admissible failure mechanism. The total force on the boundary S can be calculated only if velocity v_i on this boundary is constant. If the geometry of the structure is given and all loads and material parameters are known, the safety factor can be obtained. Earthquake effects are considered in terms of seismic coefficient-dependent horizontal forces. Only a log-spiral failure surface passing through the toe of the slope as show in Figure 1 is considered in this study.

A potential log-spiral failure surface *bd* in two dimensions is represented by the equation

$$r = r_0 e^{\alpha \tan\phi} \tag{3}$$

Where r_o is the initial radius of the log-spiral; and ϕ is the angle of soil shearing resistance. The log-spiral intersects the back slope at right angle at a distance S from point 'a'. The centre of log-spiral lies on the line *od* making angle ϕ with horizontal and α is the angle of log-spiral.

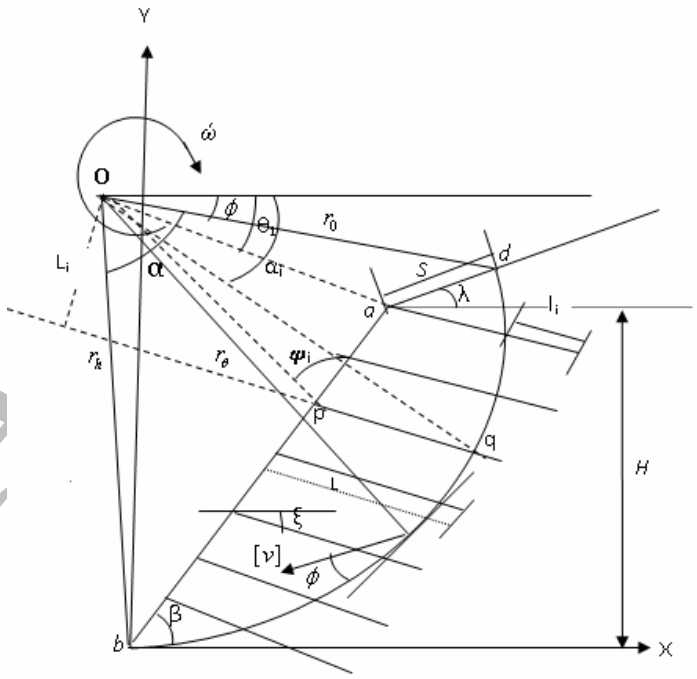

Figure 1. Log-spiral failure surface

Earthquake effect is approximated by a horizontal force equal to the product of weight of soil mass and horizontal coefficient of earthquake, acting through the center of gravity of the soil mass. In this failure mode, the reinforced soil mass above the failure surface rotates as a rigid body about the centre of rotation with angular velocity $\dot{\omega}$. The rate of work done due to soil weight and inertia force is given as (Chang et al.[12]),

$$\dot{W} = \gamma r_0^3 \dot{\omega}\left[(f_1 - f_2 - f_3) + k_h(f_4 - f_5 - f_6)\right] \tag{4}$$

Where k_h =seismic coefficient; γ = soil unit weight; and the functions f_1 through f_6 can be found in several works and are also reported in the appendix.

The rate of dissipation of internal energy due to cohesion of soil occurs along the discontinuity surface *bd*. The differential rate of dissipation of energy along the surface may be found by multiplying the differential area ($\frac{rd\theta}{\cos\phi}$), of the surface by the cohesion c and the tangential discontinuity in velocity, $v\cos\phi$ across the surface. The total internal dissipation of energy due to cohesion of soil is found by integration over the whole surface as

$$\int_0^{\alpha} c(v\cos\phi)\frac{rd\theta}{\cos\phi} = \frac{cr_o^2\dot{\omega}}{2\tan\phi}\left\{\exp\left[2(\alpha)\tan\phi\right]-1\right\} \tag{5}$$

The reinforcement contributes to the stability of the structures only through its tensile strength (reinforcement resistance to shear, torsion and bending are neglected). The kinematics requires that the velocity jump vector [v] be inclined to the velocity discontinuity at an angle of internal friction ϕ.

The energy dissipation rate during rotational failure due to the pull out resistance of reinforcement can be written as

$$\dot{D} = \dot{\omega} r_0 \sum_{i=1}^{n} T_i L_i \tag{6}$$

Where L_i is the perpendicular depth of i^{th} reinforcement layer measured downwards from the center of rotation; n is the number of the reinforcement layers; T_i is the pullout resistance force of the i^{th} layer per horizontal spacing.

The angle α_i *can* be solved by trial method from the relation

$$e^{\alpha_i \tan\phi}\{\sin(\phi+\alpha_i-\xi) = \frac{\sin(\phi+\theta_1+\beta)\times\sin(\phi+\xi)\times\sin(\beta+\phi+\xi)}{\sin\phi\times\sin(\phi+\theta_1+\xi)} \tag{7}$$

Now *pq* can be expressed as

$$pq = \frac{r_0 e^{\alpha_i \tan\phi}\times\sin(\varphi_i+\beta+\alpha_i+\phi)}{\sin(\varphi_i+\beta+\xi)} \tag{8}$$

The length l_i of i^{th} nail beyond the failure can now be found as

$$l_i = L - pq \tag{9}$$

$$L_i = r_0 e^{\alpha_i \tan\phi}\times\sin(\phi+\alpha_i-\xi) \tag{10}$$

$$T_i = (c + \sigma_{ni} \tan\delta)\frac{p_e l_i}{S_H} \tag{11}$$

or $$T_i = f^* p_e l_i / S_H \tag{12}$$

Where f^* is the limit bond stress of the soil nail interface. It is obtained from the pull out tests. l_i is anchorage length of i^{th} layer beyond the failure surface and δ is the soil-reinforcement interface angle. P_i is the perimeter of i^{th} nail; σ_{ni} is the normal vertical stress at the mid depth of i^{th} nail layer and may be expressed as

$$\sigma_{ni} = \gamma(i - \tfrac{1}{2})S_V \tag{13}$$

$$\delta = \tfrac{2}{3}\phi \tag{14}$$

Now total internal energy dissipation rate due to the cohesion of soil and tensile reinforcement force can be expressed as

$$\dot{\omega} r_0 \left[\frac{cr_0}{2\tan\phi}\{\exp[2(\alpha)]\tan\phi] - 1\} + \sum_{i=1}^{n} T_i L_i \right] \tag{15}$$

The expression for the normalized required force to maintain the equilibrium can be obtained by equating the rate of energy dissipation to the rate of work done, given as

$$K = \frac{\gamma r_0^{\,2}\{(f_1 - f_2 - f_3) + k_h(f_4 - f_5 - f_6)\} - \frac{cr_0}{2\tan\phi}\left[\exp\{2(\alpha)\tan\phi\} - 1\right]}{\sum_{i=1}^{n}[T_i L_i]} \tag{16}$$

This expression provides a lower-bound solution for the reinforcement force necessary to prevent slope failure. In order to find the best estimation of K an optimization procedure needs to be used to maximize K with respect to α. Once these angles are found, the geometry of the failure surface is completely defined.

The factor of safety F_s is calculated by taking ratio of Eq. (15) and Eq. (4), as given by

$$F_s = \frac{\frac{cr_0}{2\tan\phi}\left\{\exp\left[2(\alpha)\tan\phi\right] - 1\right\} + \sum_{i=1}^{n} T_i L_i}{\gamma r_0^2\left\{(f_1 - f_2 - f_3) + k_h(f_4 - f_5 - f_6)\right\}} \tag{17}$$

It may be observed from the above equation that the factor of safety for a given slope is a function of parameters such as angle α, r_0, height of slope H and S (the distance between the failure surface at the top of the slope and the edge of the slope). Thus minimum value of F_s

can be found using the minimization technique.

The kinematic theorem can be applied again to find the upper-bound solution for the yield acceleration factor of the log-spiral failure mechanism given as

$$K_y = \frac{\sum_{i=1}^{n} T_i L_i + \frac{cr_0}{2\tan\phi}[\exp\{2(\alpha)\tan\phi\} - 1] - r_0^2\gamma(f_1 - f_2 - f_3)}{\gamma r_o^2(f_4 - f_5 - f_6)} \tag{18}$$

The yield acceleration is defined as the horizontal acceleration in the downhill direction required bringing the safety factor with respect to slope failure to one. The critical seismic coefficient is obtained by minimizing K_y with respect to α.

It should be noted that the above expressions are derived under the assumption that the reinforcements are firmly anchored in the soil. However, when the seismic force increases the critical failure expands into the backfill, consequently some reinforcements located at the top of the slope could be pulled out if the anchorage length is not sufficient to sustain the required force. In such case, it may be assumed that only bottom reinforcements contribute to ensure global stability of the slopes by means of their tensile resistance. Therefore, the expression for K_y becomes

$$K_y = \frac{\frac{Tu}{\gamma}\sum_{i=1}^{m} L_i + \frac{Cr_0}{2\gamma\tan\phi}[\exp\{2(\alpha)\tan\phi\} - 1] - \gamma r_0^2(f_1 - f_2 - f_3)}{\gamma r_0^2(f_4 - f_5 - f_6)} \tag{19}$$

Where m is the number of reinforcements located at the bottom, which are necessary to ensure slope stability. T_u is the tensile strength of the reinforcement. The maximum value of m can be evaluated by the relation

$$mT_u = \sum_{i=1}^{n} T_i \tag{20}$$

3.Verification of Proposed Method

3.1 Case 1

The test result reported by Sheahan et al. [13] for the Clouterre Test Wall No.1 is adopted. The Test Wall was constructed using a back fill of compacted Fountainebleau sand, having friction angle $\phi = 38^0$ and cohesion, c = 3 kPa, Unit weight $\gamma = 20$ kN/m^3. The Test Wall is 7 m high with 8 cm thick shotcrete facing having weight 13.2 kN/m. The Wall was reinforced with aluminium tubes in grout. There were seven rows of nails. The lengths of first and last nails are 6 m with 1.6 cm in diameter. Remaining nails are 8 m in length with 4 cm in diameter. The soil nails had declination angle $\alpha = 10^0$ and horizontal and vertical spacing of 1.15 m and 1 m, respectively. The Test Wall was intentionally brought to failure. The

factor of safety for various log-spiral angles is calculated and shown in Figure 2.

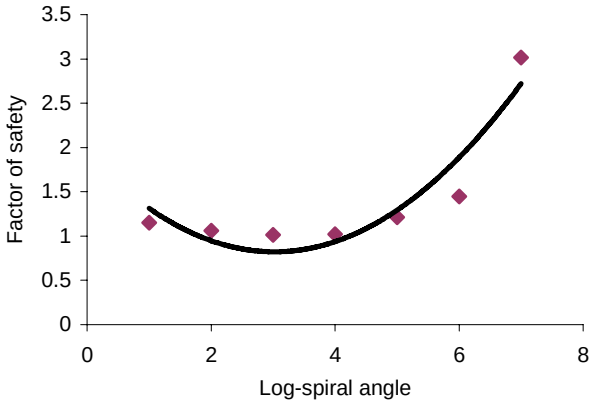

Figure 2. Variation of factor of safety with log-spiral angle (Clouterre Test Wall)

From the plot (Figure 2), the minimum value of factor of safety is obtained as 0.88. Figure 3 shows a comparison of failure surfaces obtained by present method of analysis and as observed in the field test.

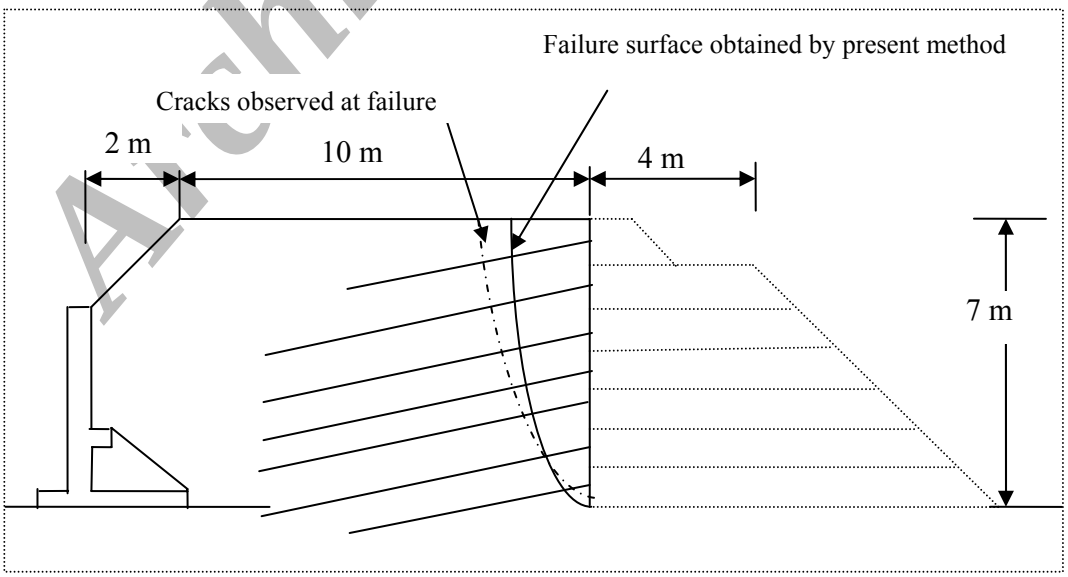

Figure 3. Comparison of failure surfaces for Clouterre Test Wall 3.1 Case 1

3.2 Case 2

The Eparris Wall of 4.5 m high, built to retain a little cut in a plastic clay is taken for the validation. The effective shear strength parameters c' and Φ' determined from a drained triaxial shear test were 0 and 28^0 respectively. The number of reinforcement layers was four, out of which the top two reinforcement layers were 4.5 m long and the bottom two were 3 m long. These reinforcements were placed from top to bottom with equal spacing and normal to the slope face. The horizontal and vertical spacing were 3 m and 1.5 m respectively. Several months after completion of the wall, during a period of heavy rains, the wall failed with kinematics indicating failure by slip of the reinforcements. The top of the wall moved away without any translation of the toe. The stability of this wall was investigated by Guiloux et al. [14] using TALREN program. The factor of safety obtained by them was 1.01.The wall is analyzed by the present method of analysis and the factor of safety is obtained as 0.99. The failure surface obtained by the TALREN program and the present method of analysis is shown in Figure 5.

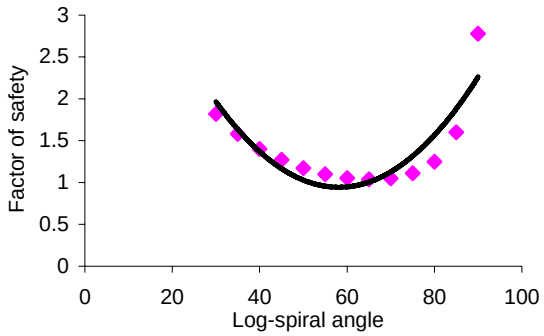

Figure 4. Variation of factor of safety with log-spiral angle (Eparris Wall)

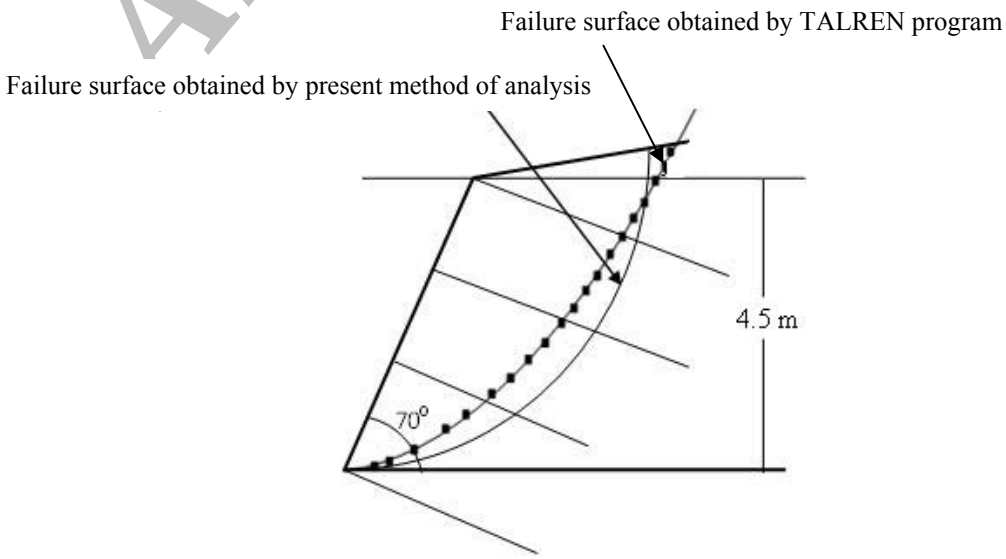

Figure 5. Comparison of failure surfaces (Eparris Wall)

3.3 Numerical analysis

The finite difference-based program FLAC (Itasca 2001) is used to develop the numerical model to simulate the two case studies. The reinforcement layers are modeled with structural (cable) elements. The concrete facing wall is assumed as rigid. The mesh and boundary condition used for two numerical models Clouterre Test Wall and Eparris Wall are shown in Figure 5 and Figure 9 respectively. The mesh size and maximum unbalanced force at the grid points are selected on a series of parametric analyses to concurrently optimize accuracy and computation speed.

The factor of safety for Clouterre Test Wall obtained by FLAC analysis is 1.18. The factor of safety as obtained by numerical analysis predicts more one, as the test wall was intentionally brought to fail after construction.

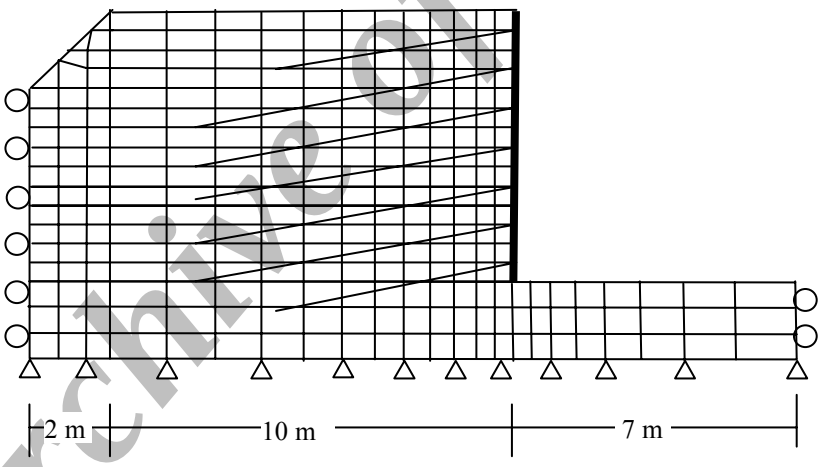

Figure 5.The mesh and boundary condition used for model Clouterre Test Wall

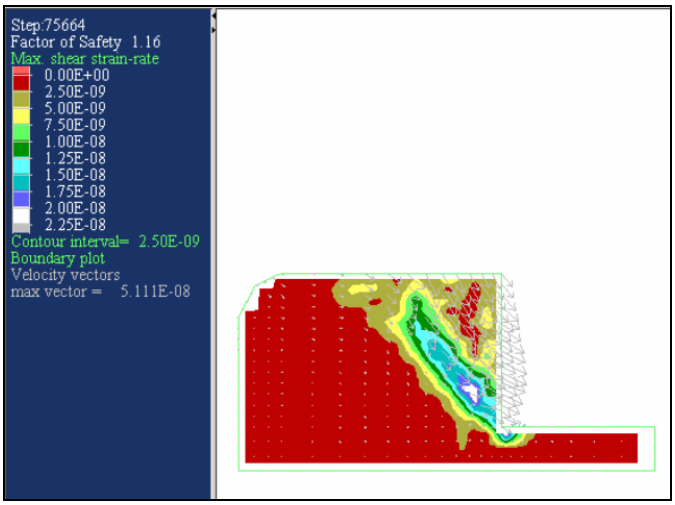

Figure 6.Factor of safety diagram of Clouterre Test Wall

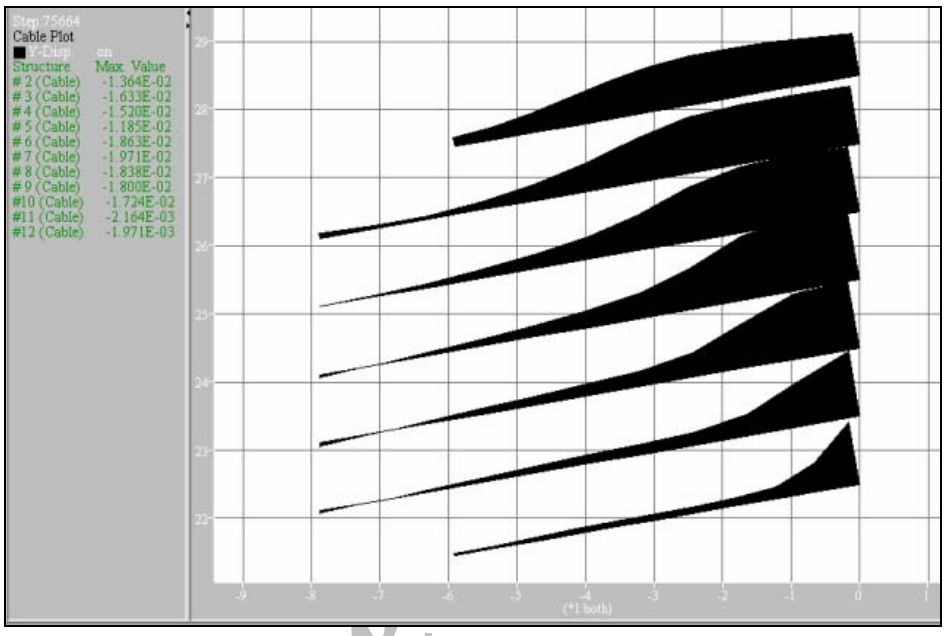

Figure 7. Y-displacement of cables

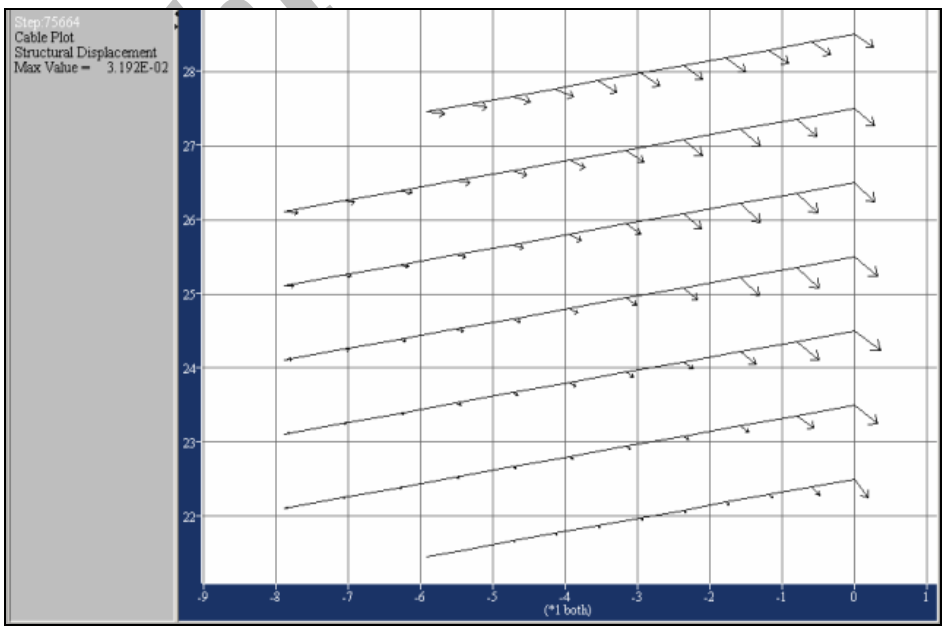

Figure 8. Structural displacement of cables

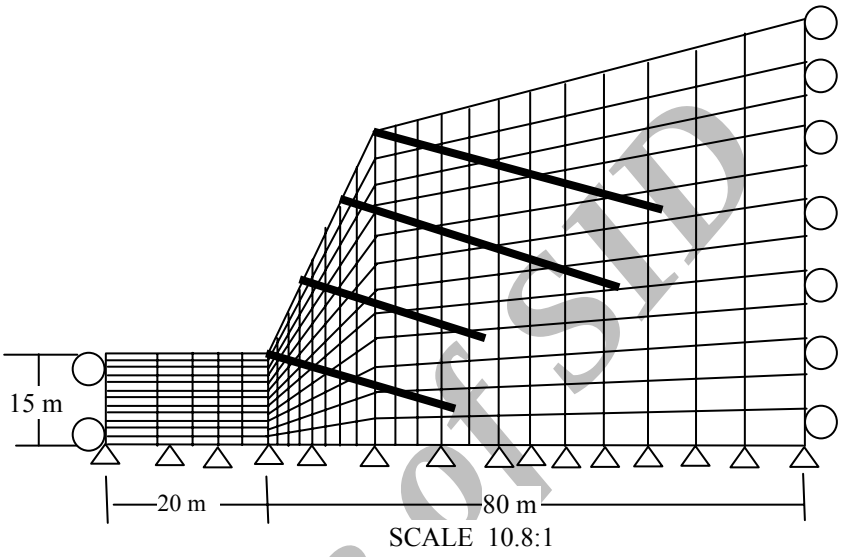

Figure 9. The mesh and boundary condition used for model Eparris Wall

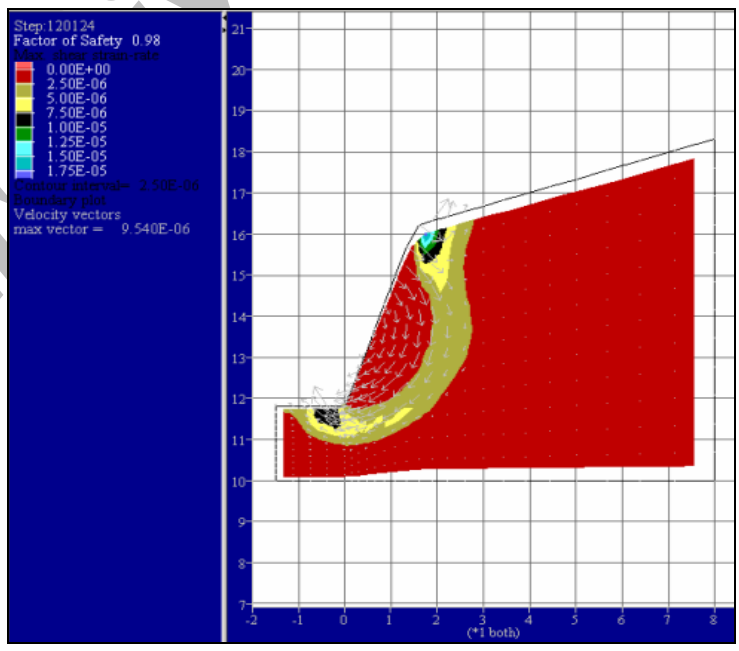

Figure 10. Factor of safety diagram of Eparris Wall

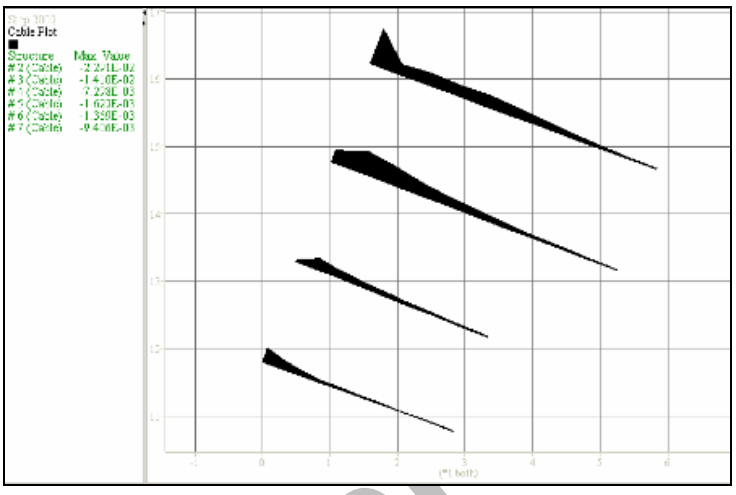

Figure 11. Y-displacement on cables.

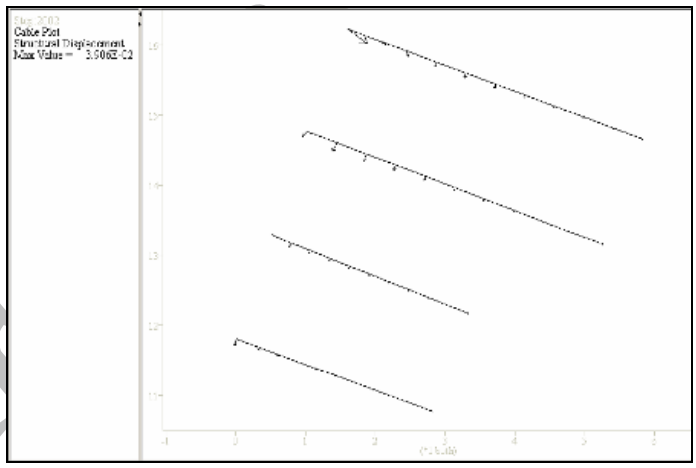

Figure 12. Structural displacement of cables.

The factor of safety of Eparris Wall obtained by numerical analysis is 0.98 which is well comparable with the value obtained by present method of analysis. The Y-displacement and structural displacement of cable are shown in Figure 11 and Figure 12 respectively. Displacement of top two nails is more which is consistency with the observed field observation as the top two nails moved away during failure of the wall.

4. Conclusion

An analytical method based on kinematical limit approach is presented for analysis of nailed soil slopes. Earthquake effects are considered in an approximate manner in terms of seismic coefficient-depended forces. The present method of analysis is used to back analyses two

published results, Clouterre Test Wall and Eparris Wall. The factor of safety obtained from the present method is in good agreement with those determined by the local minimum factor of safety method and finite element based method. The predicted slip surface by the present method is also in good agreement with the field observation crack.

Ackowledgement: The first author is grateful to the sponsored authority, Institute of Technical Education and Research, Bhubaneswar.

References

1. Stocker ME, Korcber GW, Gassler G, Gudehus G. Soil Nailing, *International conference on Soil Reinforcement*, Paris, 1979, pp. 469-74.
2. Mitchell JK, Villet WCB. Reinforcement of Earth Slopes and Embankment. National Cooperative Highway Research Program Report, Transportation Research Board, 1980,pp. 290.
3. Gassler G, Gudehus G. Soil nailing-some aspects of new technique, *Proceedings of Tenth ICSMFE*, Stockhom, 1981, pp. 665-70.
4. Gassler G. Soil nailing-Theoretical basis and practical design. *Proceedings in. Geotechnical Symposium Theory and Practice of Earth Reinforcement*, Japan, 1988, pp. 283-88.
5. Schlosser F. Behavior and design of soil nailing, Proceedings in. Symposium on. Recent Development in Ground Improvement Techniques, Bangkok, 1982, pp. 399-413.
6. Dawson EM, Roth WH, Drescher A. Slope stability analysis by strength reduction, *Geotechnique*, No. 6, **49**(1999)835-40.
7. Griffiths DV, Lane PA. Slope stability analysis by finite elements, *Geotechnique*, No. 3, **49**(1999)387-403.
8. Juran I, George B, Khalid F, Elias V. Kinematical limit analysis approach for the design of nailed soil retaining structures, *Proceedings Geotechnical Symposium on Theory and Practice of Earth Reinforcement*, Japan, 1988, pp. 301-6.
9. Juran I, George B, Khalid F, Elias V. Kinematical limit analysis approach for the design of soil nailed structures, *Journal of Geotechnical. Engineering*, *ASCE*, No. 1, **116**(1990)54-71.
10. Michalowski RL. Soil Reinforcement for Seismic design of geotechnical structures, *Computers and Geotechnics* , **23**(1998)1-17.
11. Drucker DC, Prager W, Greenberg HT. Extended limit design theorems for continuous media, *Quarterly of Applied Mathematics*, No. 4, **9**(1952)381-89.
12. Chang C, Chen WF, Yao JTP. Seismic displacements in slopes by limit analysis. J. Geotech. Engg. No. 7, **110**(1984)860-874.
13. Sheahan TC, Ho CL. Simplified trial wedge for soil nailed wall analysis, *Journal of Geotechnical and Geoenvironmental Engineering*, *ASCE*, No. 2, **129**(2003)117-24.
14. Guilloux A, Notte G, Gonin H. Experiences on retaining a structure by nailing in marine soils, *Proceeding of 8th Europan Conference on Soil Mechanics and*

Foundation Engineering, Helsinki, **2**(1983)499-502.

Notations

Basic SI units are given in parentheses.

c cohesion of soil (N/m2)
Fs factor of safety (dimensionless)
H height of slope (m)
K_h horizontal seismic acceleration coefficient (dimensionless)
K normalized required force
n number of reinforcement layers (dimensionless)
T_i pullout resistance strength of reinforce per horizontal spacing (N/m)
[v] velocity jump vector (dimensionless)
β slope angle (degrees)
Φ soil friction angle (degrees)
α angle of log-spiral
λ non negative scalar multiplier (dimensionless)
ἑ strain rate (dimensionless)
γ unit weight of soil (kN/m)
ώ angular velocity of rotation (rad/s)

Appendix

$$f_1 = \frac{\left\{\left(3\tan\phi\cos(\alpha+\phi)+\sin(\alpha+\phi)\right)\exp[3(\alpha)\tan\phi]-2\sin\phi\right\}}{3(1+9\tan^2\phi)}$$

$$f_2 = \frac{1}{6}\frac{S}{r_0}\left(2\cos\phi-\frac{S}{r_0}\cos\lambda\right)\sin(\phi+\lambda)$$

$$f_3 = \frac{1}{6}\exp[(\alpha)\tan\phi]\left[\sin\alpha-\tfrac{S}{r_0}\sin(\phi+\alpha+\lambda)\right]\times\left\{\cos\phi-\tfrac{S}{r_0}\cos\lambda+\cos(\phi+\alpha+\lambda)\exp[\alpha\tan\phi]\right\}$$

$$f_4 = \frac{1}{3(1+9\tan^2\phi)}\left\{\left(3\tan\phi\sin(\alpha+\phi)-\cos(\alpha+\phi)\right)\exp[3\alpha\tan\phi]-3\tan\phi\sin\phi+\cos\phi\right\}$$

$$f_5 = \frac{1}{3}\frac{S}{r_0}\sin^2(\phi+\lambda)$$

$$f_6 = \frac{1}{6}\exp[\alpha\tan\phi]\left[\sin\alpha-\tfrac{S}{r_0}\sin(\phi+\alpha+\lambda)\right]\times\left\{\sin\phi+\sin(\alpha+\phi)\exp[\alpha\tan\phi]\right\}$$